Effects of pressure on the fragile nature of fluorozirconates studied by molecular dynamics simulations

Yoshinori Tamai*
Department of Applied Physics, Faculty of Engineering, Fukui University, Fukui 910-8507, Japan
(Received 11 November 2002; published 25 March 2003)

Molecular dynamics simulations for a multicomponent zirconium fluoride, ZBEN ($55ZrF_4$-$17BaF_2$-$5EuF_3$-23NaF) have been carried out at various temperatures and pressures including those of the molten and glassy states. The effect of pressure on the fragile nature of ZBEN was investigated. The relaxation times were calculated from the decay curves of the intermediate scattering function. The fragile nature of ZBEN was reflected by the obvious non-Arrhenius behavior in the temperature dependence of the relaxation time. The so-called ''Angell plot'' of the relaxation time was represented by a single curve irrespective of applied pressure; the fragile nature changes negligibly with pressure. This seems to contradict the enhancement of the connectivity of ZrF_n polyhedra under high pressure. The origin of the pressure effects is discussed in comparison with those for molecular liquids and covalent-network glasses.

DOI: 10.1103/PhysRevE.67.031504 PACS number(s): 64.70.Pf, 61.20.Lc, 61.20.Ja, 62.50.+p

I. INTRODUCTION

Multicomponent zirconium fluoride systems are known as fragile glass formers. These melts have clear non-Arrhenius relaxation properties; the temperature dependence of the viscosity (and relaxation time) is described by the Vogel-Tammann-Fulcher (VTF) equation. The origin of the fragile nature has long been investigated experimentally and theoretically, as reported in detail in review articles [1–4]. The energy landscape formalism was partly successful in interpreting the phenomenology of supercooling and glass formation. However, the fragile nature is not yet fully understood. From a practical point of view, it is important to understand and control the fragile nature of these systems since the fragility affects the glass-forming processes and the stability of glass at high temperature or under extremely high pressure.

The relaxation behavior of fluorozirconate glass under high pressure is of interest. After the glass is treated under high pressures, increases in density are observed even after removal of the applied pressures; the glass is permanently densified. In the high-pressure experiments on multicomponent fluorozirconate glasses ZBE ($60ZrF_4$-$30BaF_2$-$10EuF_3$) [5] and ZBEN ($55ZrF_4$-$17BaF_2$-$5EuF_3$-23NaF) [6], the treatment-pressure dependences of the densities of permanently densified glasses exhibit maxima at 3 GPa and then marked decreases with increasing treatment pressure. Such a peculiar behavior has not been reported for the permanent densification of ''strong'' glass-forming systems such as oxide or chalcogenide glass, whose densities increase with increasing treatment pressure [7–15].

In the previous studies [16–18], the mechanism of the permanent densification of ZBEN glass was investigated by molecular dynamics (MD) simulation. The structures obtained under high pressure were decompressed at various temperatures including the glass transition temperature T_g [16]. In a particular range of the temperatures, the peculiar permanent-densification behavior was well reproduced. The fragile nature, which was manifested by the non-Arrhenius behavior of the diffusion coefficients of ions, was found to play an important role in the structural relaxation during the decompression process. The structural changes in the process of the permanent densification have also been analyzed in detail [17]. The partial preservation of the connectivity of the network-forming ZrF_n and EuF_n polyhedra causes maxima in the treatment-pressure dependencies of the structural relaxation in the F^- coordination environments around the network-modifying Ba^{2+} and Na^+ ions. The compression-decompression process under the glassy state was also mimicked by the simulation; the behavior was related to the pressure-induced phase transition of model crystals, BaF_2 and NaF [18]. The high pressure behavior of the ZBEN glass can be interpreted by the fragility and the variation of the network connectivity.

Some liquids are known to change their fragility according to their environments. Pure water is a fragile liquid at ambient temperature and pressure [19]. Water molecules coexisting with polypeptide, however, have a different temperature dependence of relaxation time of rotational motion and are considered to be rather strong liquids [20]. Angell suggested that this type of behavior may be common to all hydrophilic polymers and hence, to a large number of biopolymer systems [19]. This hypothesis has also been proved for the synthetic poly(vinyl alcohol) hydrogel by MD simulation [21]. Furthermore, a low-temperature phase of supercooled water, water II, is a strong liquid [1]. The decrease of fragility of water is accompanied by the enhancement of the regular network structures.

By compressing the fragile ZBEN glass, the enhancement of the connectivity of ZrF_n polyhedra was observed in MD simulation [17,18]. There is a possibility that the potential energy landscape varies with applied pressure. It is, however, uncertain whether or not the fragile nature of zirconium fluorides changes with pressure. There are no experimental findings concerning this issue so far because of the difficulty of

*Email address: tamai@polymer.apphy.fukui-u.ac.jp

TABLE I. Potential parameters.

Ions	z	a (Å)	b (Å)
Zr^{4+}	+4	1.380	0.072
Eu^{3+}	+3	1.510	0.075
Ba^{2+}	+2	1.800	0.077
Na^{+}	+1	1.260	0.080
F^{-}	−1	1.500	0.090

TABLE II. Sampling times of long MD simulation runs (ns).

T (K)	P_0	3 GPa	12 GPa	20 GPa	50 GPa
7000					0.2
6000				0.2	0.2
5000	0.2	0.2	0.2	0.2	0.2
4000	0.2	0.2	0.2	0.2	0.5
3500	0.2	0.2	0.2	0.5	5
3000	0.2	0.2	0.5	5	10
2500	0.2	0.5	5	10	10
2200	0.5	5	10	10	
2000	5	10	10		
1800	10	10			
1600	10				

performing high-pressure measurements of viscosity and relaxation time for ionic liquids. There have been a few experimental studies on the pressure-dependent viscosity of molecular liquids [22,23]. The fragility of glycerol, an intermediate strength liquid, increases with pressure. However, the reason for this fragility change with pressure remains an open question [23]. The enhancement of hydrogen bonding contradicts the increase in fragility under high pressure, since the network liquid SiO_2 is known to be at the extreme limit of strength in the strong-fragile classification scheme.

This paper presents the investigation of the effects of pressure on the fragile nature of fluorozirconate glass and melt by MD simulation. The fragility of the ZBEN glass has already been partly discussed in the previous study [16], based on the self-diffusion coefficient, which can be related to the viscosity by the Stokes-Einstein relation. The fragile nature of ZBEN was qualitatively manifested by the deviation from the Arrhenius law. It is, however, uncertain whether or not the Stokes-Einstein relation is really valid for ZBEN. Because of the large scatter of T_g, which was caused by the higher and nonuniform cooling rates, a definitive analysis on the pressure dependence of the fragility could not be attained in the previous study. In this study, the fragile nature is analyzed in terms of the so-called ''Angell plot'' [1] of the relaxation time, which can be directly related to the fragility. The T_g values under various pressures are carefully determined and are used as the reference temperatures of the analysis.

II. MD SIMULATIONS

The composition of ions in the MD simulation is same as that of ZBEN in the high-pressure experiment [6] and also that in the previous simulation study [16–18]. The numbers of Zr^{4+}, Ba^{2+}, Eu^{3+}, Na^{+}, and F^{-} ions contained in a cubic unit cell are 140, 43, 13, 59, and 744, respectively. A total of 999 ions were confined under the periodic boundary condition. The Busing-Ida-Gilbert potential function $U_{ij}(r_{ij})$ is used in the simulation:

$$U_{ij}(r_{ij}) = \frac{z_i z_j e^2}{r_{ij}} + f_0(b_i + b_j)\exp\left(\frac{a_i + a_j - r_{ij}}{b_i + b_j}\right), \quad (1)$$

where r_{ij} is the distance between ions i and j, z_i is the charge of ion i, a_i and b_i are the size and softness parameters, respectively, and f_0 ($=1$ kcal/mol Å$=6.9511\times10^{-11}$ N) is a constant for unit translation. Table I lists the potential parameters, which are the same as those in the previous study [16–18]. The parameters were determined by Takahashi *et al.* [24] so as to reproduce structures of model crystals (fluorides and chlorides) under ambient pressure P_0 ($=0.0001$ GPa). The applicability of these potential parameters to MD simulations under high pressures was previously confirmed [16–18]. The structures of the high pressure polymorphs of model crystals were satisfactorily reproduced by the potential model. For the highly ionic systems treated in this study, it is justifiable to apply the present potential parameters to MD simulations under high pressure.

The initial positions of ions were generated randomly by using a Monte Carlo-like scheme, in which severe overlap of ions was avoided. MD simulations were performed for ZBEN melt and glass in the temperature range 300–7000 K and pressure range 0.0001–50 GPa. The long-range Coulomb interactions were handled by the Ewald sum method [25]. Temperatures and pressures were controlled by the Nosé-Andersen constant temperature-pressure method [26,27]. The virtual masses of volume and the time scaling parameter are 0.005 amu/Å^4 and 1.0×10^5 amu Å^2, respectively, which produce the fluctuation period of approximately 1 ps. The equations of motion were solved by the Verlet algorithm [25,28] with a time step of 1 fs, which is sufficiently short for the conservation of the Hamiltonian even at the highest temperature in the present simulation.

An equilibrated ZBEN structure was obtained by MD simulation of 0.3 ns at 5000 K under P_0. The structure was compressed stepwise to $P=1$, 3, 6, 9, 12, 16, 20, 30, 40, and 50 GPa through simulations at 0.3 ns intervals under each P at 5000 K (compression run). The structures under P_0, 3, 12, 20, and 50 GPa were then quenched to 300 K through sequential constant N-P-T simulations at 0.3 ns intervals at every 100 K in the range of 5000–300 K (quenching run). The cooling rate was 0.33 K/ps, which was constant in all the temperature ranges. Long-time sampling runs of up to 10 ns were performed under $P=P_0$, 3, 12, 20, and 50 GPa in order to determine dynamical properties (long-time run). The sampling times of long-time runs are listed in Table II. Simulations at 6000 and 7000 K were also performed under 20 and 50 GPa for 0.3 ns using the last coordinate at 5000 K as an initial configuration. The trajectories and velocities of ions were recorded every 1000 steps on disk files for later analy-

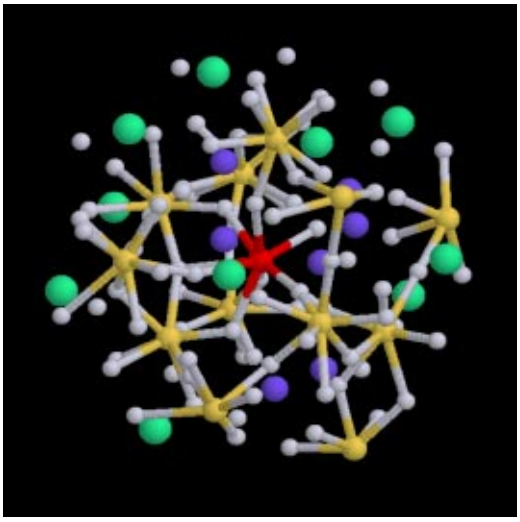

FIG. 1. (Color online) Snapshot of ZBEN glass at 1600 K under 20 GPa. Clusters in radii of 6.73 Å (114 ions) are extracted from the simulation cell. Network-forming Zr^{4+} (yellow) and Eu^{3+} (red) ions (middle-size spheres) are connected by F^- ions (white). Network-modifying Ba^{2+} (green) and Na^+ (blue) ions (large spheres) are surrounded by networks composed of ZrF_n and EuF_n polyhedra.

ses. Furthermore, in order to measure rapid-motion time correlation functions, short-time constant *N-V-T* MD simulations (2–25 ps), in which the trajectories were recorded every 1–5 steps, were also performed using the last coordinates of the long-time runs as initial structures (short-time run).

MD simulations were performed on a CRAY Origin 2000 parallel computer at the Human Genome Center, Institute of Medical Science, University of Tokyo. The molecular simulation program PAMPS [29] coded and developed by the author was used for all calculations.

III. RESULTS AND DISCUSSION

A. Structure of ZBEN glass

Figure 1 shows the snapshot of the ZBEN glass at 1600 K under 20 GPa. A cluster of 114 ions around Eu^{3+} ions was extracted from the unit cell. The network-forming Zr^{4+} and Eu^{3+} ions construct the three-dimensional network structures in combination with F^- ions. The network-modifying Ba^{2+} and Na^+ ions uniformly distribute in the networks composed of the ZrF_n and EuF_n polyhedra. The average coordination number of F^- ions, n, around the Zr^{4+} and Eu^{3+} ions are 8–9. Most of the ZrF_n polyhedra are connected by sharing their corners (sharing one F^- ion) and some of the polyhedra (for example, see two polyhedra in the lower right part) share their edges (sharing two F^- ions). A quantitative analysis for these structural features are presented elsewhere [17].

B. Glass transition temperature

Figure 2 shows the temperature dependences of potential energy U and specific volume v_c in quenching runs. As is the nature of fragile liquids, the difference in the slopes between

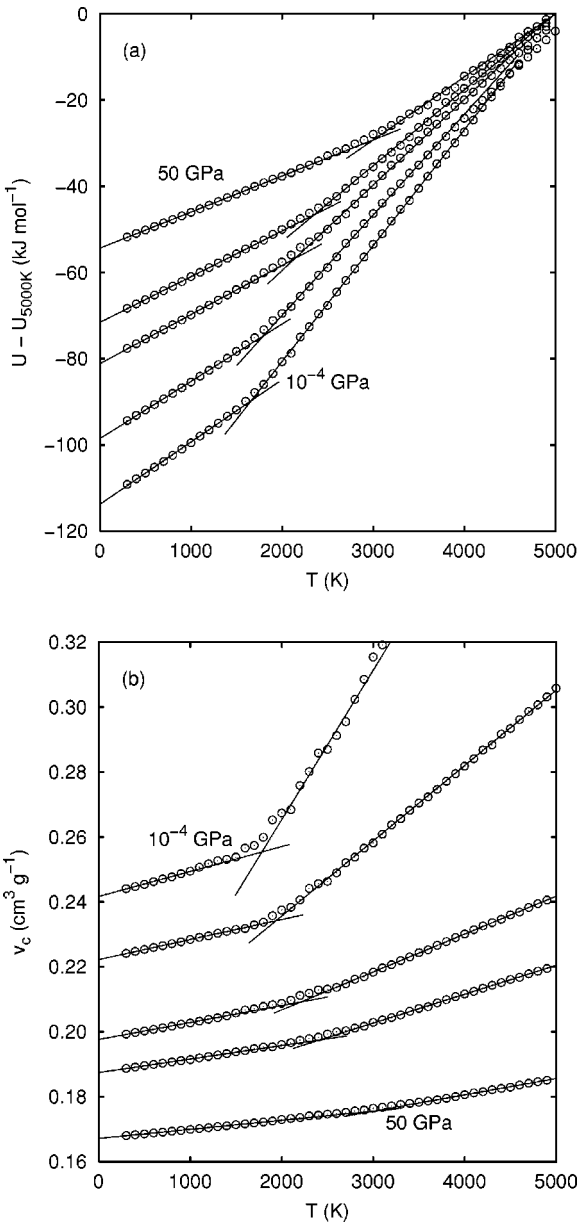

FIG. 2. Temperature dependences of (a) potential energy and (b) specific volume in quenching runs under 0.0001, 3, 12, 20, and 50 GPa.

liquid and glassy states is obvious. The glass transition temperature T_g under each P can be straightforwardly determined from the breaks in the dependences of the potential energy. As for the specific volume, however, the transformation range around T_g was observed rather wide temperature range; the slopes change gradually near T_g. In the region, the F^- ions can diffuse in the matrix though the mobility of Zr^{4+} is frozen, as shown in a later section. Note that the fluorozirconate glasses are known as F^- ion conductive materials. Several dynamical processes with different time scales coexist in the system. The T_g value was determined as the crossing point of two linear fits to the low and high temperature ranges; the fitting ranges and the obtained T_g values are listed in Table III.

The pressure dependencies of T_g, which are shown in Fig. 3, are different between those determined from the po-

TABLE III. Fitting range to determine glass transition temperature T_g, and the T_g value obtained by fitting.

P (GPa)	T_2^{LT} (K)[a]	T_1^{HT} (K)[b]	T_g (K)
	Potential energy		
0.0001	1500	1800	1660
3	1500	2100	1800
12	1700	2300	2140
20	1900	2500	2350
50	2000	3100	3000
	Specific volume		
0.0001	1000	2000	1780
3	1500	2200	1940
12	1500	2800	2210
20	1700	3100	2420
50	1900	3600	2990

[a]Upper limit of fitting in low temperature region.
[b]Lower limit of fitting in high temperature region.

tential energy and those determined from the specific volume. Hereafter, the former is called T_g and the latter is called T_g^v. The latter is affected by the transformation range. The T_g value increases with applied pressure because of the decrease in the moving space for ions under high pressure, as is experimentally observed for other systems [30]. The curve of $T_g(P)$ is nonlinear with pressure. The nonlinearity of $T_g(P)$ was also observed in experimental studies of several fragile glasses and molecular liquids [22,23]. The calculated value of dT_g/dP is approximately 30 K/GPa, the same order as the experimentally estimated value $\sim$80 K/GPa for fluorozirconate glass $53ZrF_4$-$20BaF_2$-$4LaF_3$-$3AlF_3$-20NaF [31].

The T_g value under ambient pressure P_0 is $\approx$1600 K, which is much higher than the experimental one of $\sim$520 K [6]. This can be attributed partly to the difference in cooling rates between the experiment and simulation. The main source of the discrepancy is attributed to the simple point charge models that have been widely used in the simulation of inorganic materials. In the precise simulation study of

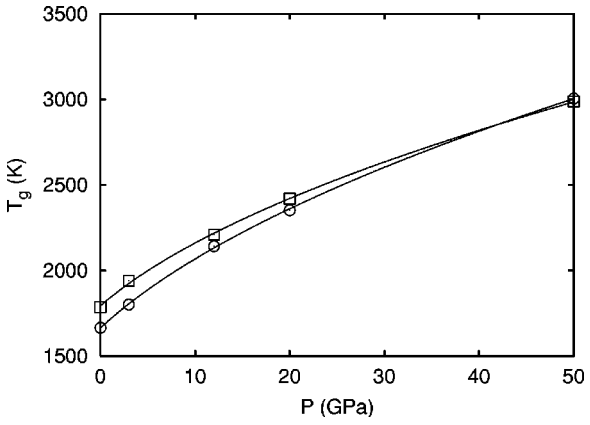

FIG. 3. Pressure dependence of glass transition temperatures T_g, which were obtained from breaks in the temperature dependence of potential energy ($\bigcirc$) and specific volume ($\square$). The solid curve is a guide to the eye.

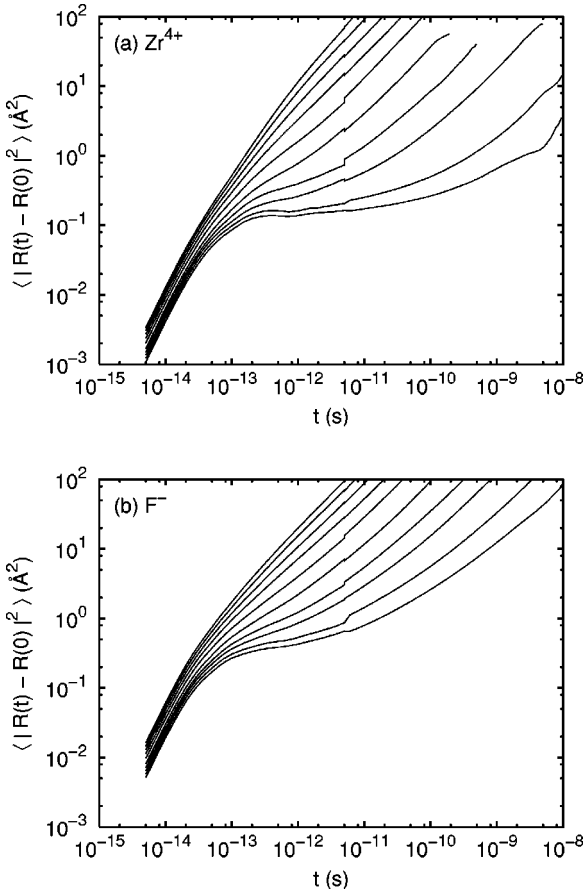

FIG. 4. Mean-square displacements of (a) Zr^{4+} and (b) F^- ions under P_0 at various temperatures: 5000, 4500, 4000, 3500, 3000, 2500, 2200, 2000, 1800, and 1600 K from upper to lower lines. The curves of MSD for short- and long-time runs are joined at $t=5\times10^{-12}$ s.

cooling-rate effects in amorphous silica [32], in which a potential function similar to Eq. (1) was used, the T_g values were calculated to be 2900–3300 K, and thus were more than two times higher than the experimental value of 1446 K. Although several potential functions such as Eq. (1) and parameter sets for amorphous silica have been tested, the calculated T_g values are around 3000 K [33]. The melting temperatures of the model crystals ZrF_4, EuF_3, BaF_2, and NaF, whose structures were well reproduced under P_0 [16], were calculated to be 4800, 2800, 2200, and 2000 K, respectively [33], using the potential parameters in Table I. These values are also approximately two times higher than experimental values.

One may overcome the discrepancy by incorporating a many-body interaction into the potential function, and updating the potential function and parameters at every time step according to the ion configurations. This, however, costs exhaustive amounts of computation time. In the simulation of supercooled liquids and glasses, it is most important to simulate the system for as long as possible, because the relaxation time becomes exceedingly long. Using the present potential functions [Eq. (1)] and parameters (Table I), the structures of the model crystals under P_0 were well reproduced. Furthermore, high-pressure polymorphs of BaF_2 and NaF were also

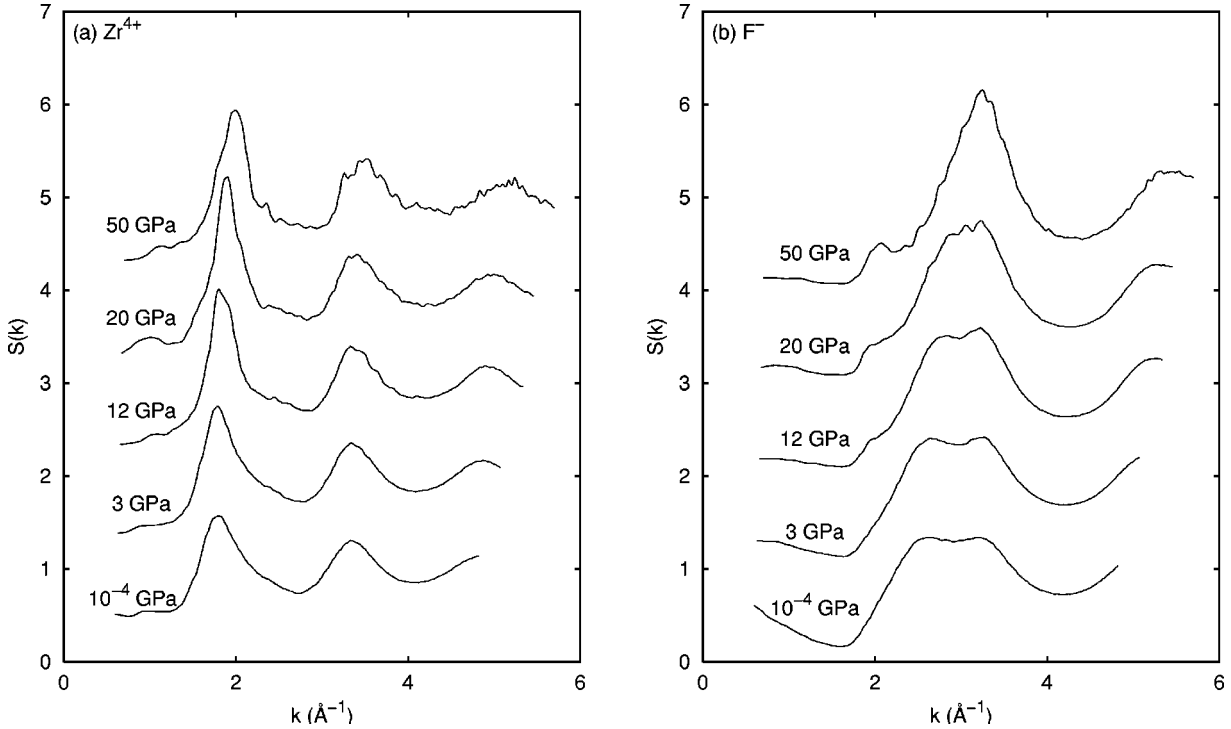

FIG. 5. Static structure factor $S(k)$ at 2500 K: (a) Zr^{4+} and (b) F^- ions in ZBEN.

well reproduced under high pressure, and pressure-induced phase transition was also demonstrated [18]. Considering the trade-off, I decided that long-time MD simulations should be performed using the present potential functions; the relaxation process should be analyzed in terms of normalized temperatures T/T_g, which are based on the calculated T_g values in the simulation.

Although the T_g values are much higher, the present model provides the physical essences of the real ZBEN glass: the large difference in mobility between Zr^{4+} and F^- ions, the differences in the coordination environments between the network-forming ions (Zr^{4+} and Eu^{3+}) and network-modifying ions (Ba^{2+} and Na^{4+}) [17], the structures of the low- and high-pressure polymorphs of model crystals, and the pressure induced structural phase transition between these polymorphs [18]. Therefore, the present simulation is reliable enough to study the relaxation process in the ZBEN glass.

C. Diffusion of ions

The mean-square displacements (MSD's) of the Zr^{4+} and F^- ions were calculated. Figure 4 shows MSDs of Zr^{4+} and F^- ions in the ZBEN melt and glass under P_0. The MSD's obey Einstein's equation (increase linearly with time t) at long-time regions. The mobility of Zr^{4+} ions is rather smaller compared to F^- ions. The ZBEN glass is in the glassy state at 1600 K since the square root of MSD of the Zr^{4+} ions does not exceed $d_{\text{Zr-Zr}}/2$, where $d_{\text{Zr-Zr}}$ is the average Zr-Zr spacing, 4.2 Å, which is determined as the position of the first peak in the radial distribution function between Zr^{4+} ions. The Zr^{4+} ions are virtually arrested at 1600 K in the typical observation time of the simulation, 10^{-9} s. The F^- ions, however, diffuse normally at the temperature. The result is consistent with the fact that fluorozirconate glasses are F^- ion conductive materials.

D. Static structure factor

The static structure factor $S(\mathbf{k})$ is defined as

$$S(\mathbf{k}) = \frac{1}{N}\langle \rho_{\mathbf{k}} \rho_{-\mathbf{k}} \rangle, \tag{2}$$

where

$$\rho_{\mathbf{k}} = \int \rho(\mathbf{r}) \exp(-i\mathbf{k}\cdot\mathbf{r}) d\mathbf{r}, \tag{3}$$

$\rho(\mathbf{r}) = \Sigma_{i=1}^{N} \delta(\mathbf{r} - \mathbf{r}_i)$ is the number density at a point $\mathbf{r}$ in the volume V of the N particle system, $\mathbf{k}$ is a reciprocal vector, and $\langle \cdots \rangle$ means the ensemble average. In the molecular simulation, $S(\mathbf{k})$ can be calculated by

$$S(\mathbf{k}) = \frac{1}{N}\left\langle \left(\sum_{i=1}^{N} \cos\mathbf{k}\cdot\mathbf{r}_i \right)^2 + \left(\sum_{i=1}^{N} \sin\mathbf{k}\cdot\mathbf{r}_i \right)^2 \right\rangle, \tag{4}$$

where $\mathbf{k} = 2\pi\mathbf{h}/L$, L is the edge length of a cubic unit cell, and $\mathbf{h}$ = (1 0 0), (1 1 0), (1 1 1), (2 1 0), etc. Figure 5 shows $S(k)$ of the Zr^{4+} and F^- ions. All the reciprocal vectors $\mathbf{k}$ that satisfy $|\mathbf{k}| = k$ are included in the calculation of each point of $S(k)$. The data were smoothed by a running average method, i.e., an average of three successive columns, $[S(k_{i-1}) + S(k_i) + S(k_{i+1})]/3$, was substituted for $S(k_i)$. The procedure was repeated three times.

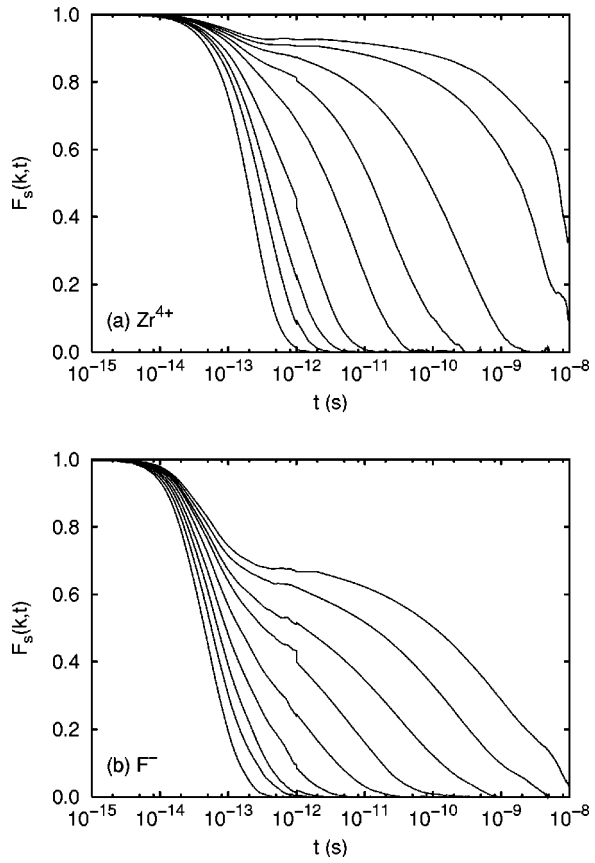

FIG. 6. Intermediate scattering function $F_s(k,t)$ at $k=k_{\max}$ for (a) Zr^{4+} and (b) F^- ions under P_0 at various temperatures: 5000, 4000, 3500, 3000, 2500, 2200, 2000, 1800, and 1600 K from lower to upper lines. The curves of $F_s(k,t)$ for short- and long-time runs are joined at $t=10^{-12}$ s.

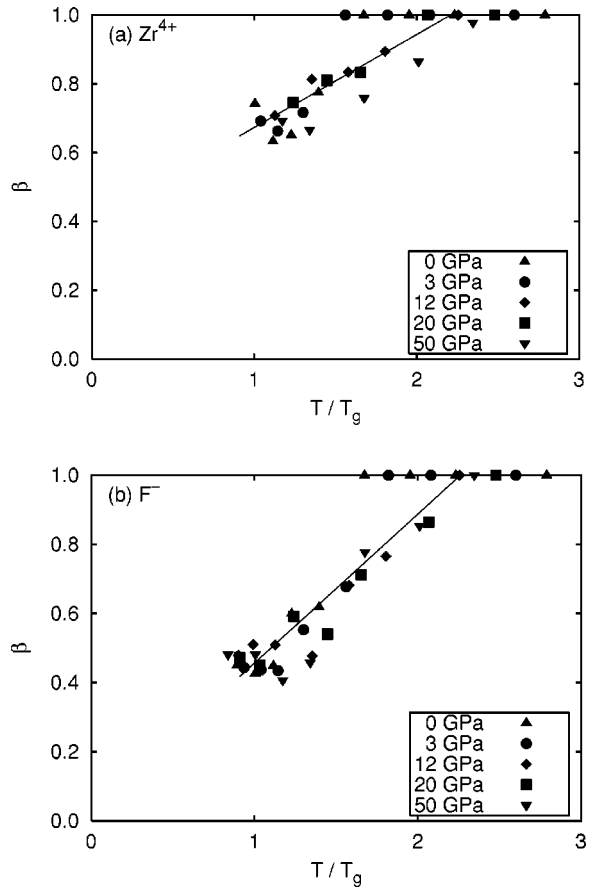

FIG. 7. Temperature dependence of stretched exponent β: (a) Zr^{4+} and (b) F^- ions in ZBEN. Temperatures are normalized by glass transition temperature T_g under each pressure. The solid line is a guide to the eye.

In the $S(k)$ curves of Zr^{4+} ions, the peak position of the first maximum, $k_{\max}$, is slightly shifted to higher values with increasing applied pressure while that of the second one is approximately constant. In the $S(k)$ curves of F^- ions, the main peak at around $k=3$ Å^{-1} splits into two maxima $k_{\max,1}=2.6$ Å^{-1} and $k_{\max,2}=3.2$ Å^{-1} at 2500 K under P_0. Although the values of $k_{\max,2}$ do not vary with P, the peak positions $k_{\max,1}$ are considerably shifted to higher values with increasing P. The $k_{\max,1}$ value coincides with $k_{\max,2}$ under $P=50$ GPa. In the previous study [17], the structure and connectivity of the ZrF_n polyhedra in ZBEN glass were investigated in detail. With increasing P, only slight changes were observed in the Zr—F bond lengths and F—Zr—F bond angles. A marked change was observed in the connectivity of the ZrF_n polyhedra; the number of corner-sharing polyhedra decreased and that of edge-sharing polyhedra increased with P. This change may be reflected in the large shifts of $k_{\max,1}$.

E. Intermediate scattering function

In order to estimate the relaxation time, the intermediate scattering function

$$F_s(\mathbf{k},t)=\langle\hat{\rho}_s(\mathbf{k},t+t_0)\hat{\rho}_s(-\mathbf{k},t_0)\rangle, \quad (5)$$

where $\hat{\rho}_s(\mathbf{k},t)=\exp[i\mathbf{k}\cdot\mathbf{r}(t)]$, was calculated. Figure 6 shows $F_s(k,t)$ of Zr^{4+} and F^- ions as a function of time for different temperatures under P_0. All the reciprocal vectors that satisfy $|\boldsymbol{k}|=k_{\max}$ (the peak position of $S(k)$ at each T under each P) were included in the calculation of $F_s(k,t)$. The first peak $k_{\max,1}$ is used in the calculation of $F_s(k,t)$ of F^- ions. The decay of $F_s(k,t)$ is clearly described by two relaxation processes. All the curves are well fitted by the following equation:

$$F_s(k,t)=(1-C)\exp(-t/\tau_s)+C\exp[-(t/\tau_l)^{\beta}], \quad (6)$$

where C, τ_s, τ_l, and β are fitting parameters. The short-time relaxation process with a time scale of $\sim\tau_s$ is described by a single exponential decay. On the other hand, the long-time one with a time scale of $\sim\tau_l$ is nonexponential. The fitting parameters were obtained from the nonlinear least-squares fit. The temperature dependences of the stretched exponent β are shown in Fig. 7. At high temperatures, the β value is unity; the decay curve is represented by a single exponential function. The β value decreases to 0.5 as the temperature is lowered towards T_g. This noteworthy nonexponential relaxation near T_g is often observed for fragile supercooled liquids.

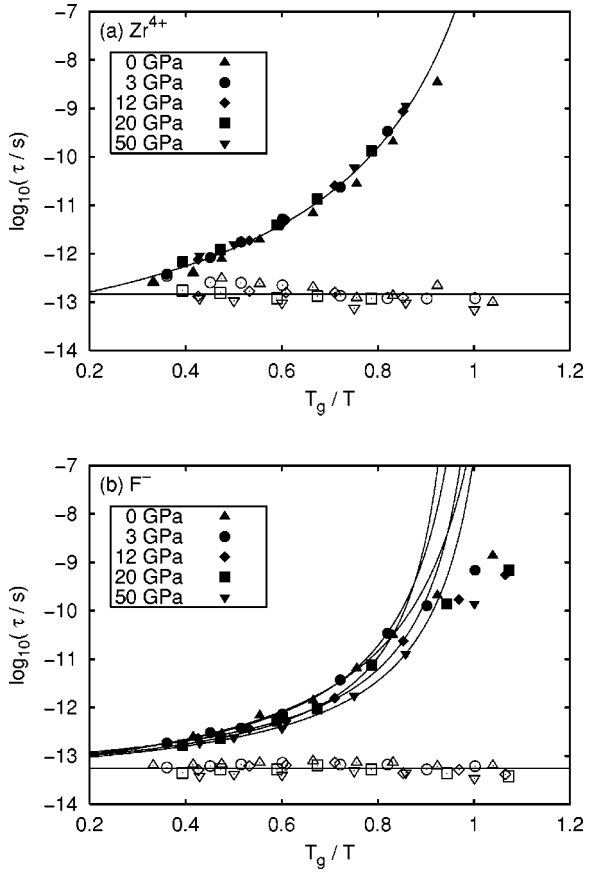

FIG. 8. Temperature dependence of relaxation times τ_s (open symbols) and τ_l (solid symbols) of (a) Zr^{4+} and (b) F^- ions in ZBEN under pressures 0.0001, 3, 12, 20, and 50 GPa. Temperatures are normalized by glass transition temperature T_g under each pressure, which was determined from the temperature dependence of "potential energy." The solid curves are fits to the VTF equation and the solid linear line is fit to the Arrhenius law.

F. Relaxation time

The long relaxation times τ_l are analyzed in terms of the Angell plot (the VTF equation) [1]

$$\ln \tau = A + \frac{DT_0}{T - T_0}, \tag{7}$$

where A, D, and T_0 are the fitting parameters. The strength parameter D becomes small for fragile liquids. The parameter T_0 is correlated with the Kauzmann temperature. Figure 8 shows the Angell plot for the Zr^{4+} and F^- ions. The temperatures were scaled by the glass transition temperatures T_g, which were determined from the temperature dependence of energy. The short relaxation times τ_s, which correspond to the β_f process, are constant at all temperatures. On the other hand, the long relaxation times τ_l increase with decreasing temperature and are well fitted to the VTF equation. The obvious non-Arrhenius behavior indicates that ZBEN is a fragile liquid, as was also manifested by the deviation from the Arrhenius law of the self-diffusion coefficient in the previous study [16].

All the τ_l values under different pressures are well described by a single curve for Zr^{4+} as shown in Fig. 8(a). In experiments, the relaxation time proves to be equivalent to the observation time of $\sim$100 s; all the curves in the Angell plot cross at $T_g/T=1$ and $\tau=100$ s [1]. Although the observation time in the present MD simulation is much shorter than the real experiments, all the curves of τ_l under different pressures coincide with one value at T_g. Therefore, the long relaxation time τ_l is a good measure of the system relaxation in the present simulation.

The deviation from the single curve is somewhat large for the τ_l values of F^- ions, as shown in Fig. 8(b). As shown in Fig. 2(b), the slopes of the specific volume change gradually with T near T_g. In this transformation range, the F^- ions can diffuse in the matrix while the mobility of Zr^{4+} is frozen. Since F^- ions disperse continuously while Zr^{4+} ions are separated from each other by F^- ions, the volume relaxation is governed by the mobility of F^- ions. Therefore, T_g^v, which was obtained from the temperature dependence of the specific volume, is suitable as the reference temperature of the relaxation of F^- ions. The Angell plot of F^- ions is shown in Fig. 9, in which temperatures were normalized by T_g^v. All the τ_l values under different pressures are clearly described by a single curve.

At $T_g/T>0.9$, the values of τ_l determined for F^- ions deviate from the VTF line and fall along the other straight line. This is not the error caused by the shortage of simulation time since the simulations were performed for sufficiently (more than 10 times) longer times than each value of τ_l. Following the theory of Adam and Gibbs [34], the temperature dependence of relaxation time is explained as

$$\tau = \tau_0 \exp\left(\frac{C}{TS_c}\right), \tag{8}$$

where τ_0 and C are constants and S_c is the configurational entropy. Since the configurational entropy of fragile liquids rapidly changes with temperature, obvious non-Arrhenius

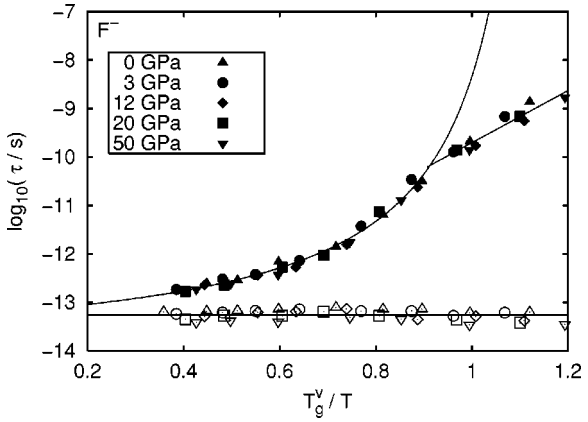

FIG. 9. Temperature dependence of relaxation times τ_s (open symbols) and τ_l (solid symbols) of F^- ions in ZBEN under pressures 0.0001, 3, 12, 20, and 50 GPa. Temperatures are normalized by glass transition temperature T_g^v under each pressure, which was determined from the temperature dependence of "specific volume."

behavior is observed. If S_c is frozen at T_g, however, the Arrhenius law becomes applicable to τ. In the present system, the α-relaxation process is dominated by the relaxation of the network structures of ZrF_n polyhedra. The relaxation time τ_l calculated for Zr^{4+} ions increases excessively near T_g, as shown in Fig. 8(a). Although the network structures are frozen below T_g, the F^- ions can diffuse in the networks. Note that the fluorozirconate glasses are known as F^- ion conductive materials. The diffusional motion of F^- ions in the frozen networks obeys the Arrhenius law, as is clearly seen in Fig. 9.

G. Pressure dependence of fragility

As shown in Figs. 8(a) and 9, the values of τ_l under different pressures fall onto a single line. The parameters of A, D, and T_0 were obtained by the nonlinear least-squares fit. The small values of strength parameters D, 4.5 and 2.1, calculated for Zr^{4+} and F^- ions, respectively, indicate that ZBEN is a fragile liquid. The most noteworthy finding is that the D values do not depend on pressure. The fragile nature negligibly changes with pressure in spite of differences in the connectivity of ZrF_n polyhedra. Contrary the pressure-driven change in fragility was examined experimentally for glycerol, a hydrogen-bonded molecular liquid [23]. At ambient pressure, glycerol is an intermediate strength liquid ($D=17$). At high pressure, glycerol becomes almost as fragile as orthoterphenyl, one of the most fragile liquids known; the value of D decreases to 3 at 3 GPa. The hydrogen-bonding networks in glycerol increase at high pressures, as interpreted from high-pressure NMR chemical shift data [35]. The connectivity of ZrF_n polyhedra in ZBEN is also enhanced under high pressure, as shown in the previous study [17]. The fraction of edge-sharing ZrF_n polyhedra increases from 5% (under P_0) to 20% (under 20 GPa), while the fraction of corner-sharing ones decreases. Since the ZBEN melt under P_0 is originally at the extreme limit of fragility, the fragility does not increase further under high pressure.

Although the behavior of ZBEN melt is similar to that of glycerol, the results confuse the explanation of the relationship between the fragility and the network character, i.e., that glassformers of large connectivity are strong glassformers, since network liquids such as SiO_2 are known to be at the extreme limit of strength for liquids. The structural features of ionic fluorozirconate glasses are quite different from those of covalent-network glasses. In fluorozirconate glasses, chemical bonds between the glass constituent ions have an extremely high ionic character. As a result, the packing densities reach about 65%, compared with 50–55 % in oxide glasses. In addition, in crystalline fluorozirconates with known structures, the F^- coordination numbers for Zr^{4+} ions are 6, 7, and 8 [36]. It is postulated that not only strong bonds between atoms but also tetrahedral regular networks with low packing density are needed for the system to have a strong nature. SiO_2 and water II satisfy this condition, while ZBEN and glycerol do not. Further studies, for example, on the pressure dependence of fragility of SiO_2 liquids, are required to gain a comprehensive understanding of the pressure dependence of fragility.

IV. CONCLUSIONS

Molecular dynamics simulations for a multicomponent zirconium fluoride ZBEN have been carried out at various temperatures and pressures including those of the molten and glassy states. The effect of pressure on the fragile nature of ZBEN was investigated. The glass transition temperature was found to increase with pressure. The relaxation times, which were calculated from the decay curves of the intermediate scattering function $F_s(k,t)$, were analyzed in terms of the Angell plot. Obvious non-Arrhenius behavior was observed above T_g. The relaxation times obtained from $F_s(k,t)$ of F^- ions exhibited the non-Arrhenius to Arrhenius transition at around T_g. The curves of the Angell plot fall on a single line irrespective of applied pressure; the fragility does not change with pressure. Since the connectivity of ZrF_n polyhedra is enhanced under high pressure, the result seems to contradict the fact that network liquids such as SiO_2 are at the opposite extreme to fragile liquids. Not only strong bonds between atoms but also tetrahedral regular networks with low packing density are inferred to be required for liquids to have the strong nature.

ACKNOWLEDGMENTS

Generous amounts of computation time were provided by the Human Genome Center, Institute of Medical Science, University of Tokyo. The author thanks Professor Y. Kawamoto at Kobe University for helpful discussions.

[1] C.A. Angell, Science **267**, 1924 (1995).
[2] F.H. Stillinger, Science **267**, 1935 (1995).
[3] C.A. Angell, K.L. Ngai, G.B. McKenna, P.F. McMillan, and S.W. Martin, J. Appl. Phys. **88**, 3113 (2000).
[4] P.G. Debenedetti and F.H. Stillinger, Nature (London) **410**, 259 (2001).
[5] K. Miyauchi, J. Qiu, M. Shojiya, Y. Kawamoto, and N. Kitamura, Mater. Res. Bull. **34**, 1383 (1999).
[6] K. Miyauchi, M. Shojiya, Y. Kawamoto, and N. Kitamura, J. Phys. Chem. Solids **62**, 2039 (2001).
[7] P.W. Bridgman and I. Simon, J. Appl. Phys. **24**, 405 (1953).
[8] H.M. Cohen and R. Roy, J. Am. Ceram. Soc. **44**, 523 (1961).
[9] J.D. Mackenzie, J. Am. Ceram. Soc. **46**, 461 (1963).
[10] J.D. Mackenzie, J. Am. Ceram. Soc. **46**, 470 (1963).
[11] J. Arndt and D. Stöffler, Phys. Chem. Glasses **10**, 117 (1969).
[12] S. Sakka and J.D. Mackenzie, J. Non-Cryst. Solids **1**, 107 (1969).
[13] J.B. Park and D.R. Uhlmann, J. Non-Cryst. Solids **7**, 438 (1970).
[14] D.R. Uhlmann, J. Non-Cryst. Solids **13**, 89 (1973).
[15] G. Parthasarathy and E.S.R. Gopal, Bull. Mater. Sci. **7**, 271 (1985).
[16] Y. Tamai and Y. Kawamoto, J. Chem. Phys. **112**, 3875 (2000).
[17] Y. Tamai and Y. Kawamoto, Phys. Rev. B **62**, 865 (2000).

[18] Y. Tamai and Y. Kawamoto, J. Non-Cryst. Solids **306**, 282 (2002).
[19] C.A. Angell, in *Hydrogen Bond Networks*, edited by M.-C. Bellissent-Funel and J. C. Dore (Kluwer Academic, Dordrecht, 1994), pp. 3–22.
[20] J.L. Green, J. Fan, and C.A. Angell, J. Phys. Chem. **98**, 13 780 (1994).
[21] Y. Tamai and H. Tanaka, Phys. Rev. E **59**, 5647 (1999).
[22] C.A. Herbst, R.L. Cook, and H.E. King, Jr., Nature (London) **361**, 518 (1993).
[23] R.L. Cook, H.E. King, Jr., C.A. Herbst, and D.R. Herschbach, J. Chem. Phys. **100**, 5178 (1994).
[24] M. Takahashi, R. Yamamoto, R. Kanno, and Y. Kawamoto, J. Phys.: Condens. Matter **7**, 4583 (1995).
[25] M.P. Allen and D.J. Tildesley, *Computer Simulation of Liquids* (Oxford University Press, Oxford, 1987).
[26] S. Nosé, J. Chem. Phys. **81**, 511 (1984).
[27] H.C. Andersen, J. Chem. Phys. **72**, 2384 (1980).
[28] L. Verlet, Phys. Rev. **159**, 98 (1967).
[29] Y. Tamai, H. Tanaka, and K. Nakanishi, Macromolecules **27**, 4498 (1994).
[30] T. Atake and C.A. Angell, J. Phys. Chem. **83**, 3218 (1979).
[31] S. Aasland, T. Grande, A. Grzechnik, and P.F. McMillan, J. Non-Cryst. Solids **195**, 180 (1996).
[32] K. Vollmayr, W. Kob, and K. Binder, Phys. Rev. B **54**, 15 808 (1996).
[33] Y. Tamai (unpublished).
[34] G. Adam and J.H. Gibbs, J. Chem. Phys. **43**, 139 (1965).
[35] R.F. Marzke, D.P. Raffaelle, K.R. Halvorson, and G.H. Wolf, in *Second International Discussion Meeting on Relaxations in Complex Systems*, edited by K.L. Nagi (Alicante, Spain, 1993).
[36] A.F. Wells, *Structural Inorganic Chemistry*, 4th ed. (Clarendon Press, Oxford, 1975).